Observations and simulations of the formation of the faceted snow crystals in the weak-layer of the 1998 Niseko Haru no Taki avalanche.

J. McElwaine*, A. Hachikubo, M. Nemoto, T. Kaihara,
T. Yamada and K. Nishimura

Institute of Low Temperature Science,
University of Hokkaido,
North 19 West 8, Kita-Ku,
Sapporo 0060-0819, Japan

November 14, 2000

Cold Regions Science and Technology Paper No. 367

Abstract

On 28th January 1998 an avalanche accident occurred near the Japanese ski resort Niseko Alpen in Hokkaido. The following morning a snow-pit was dug through the fracture line and the snow cover analysed. There was a weak layer of faceted crystals at a depth of 1m and it was this weak layer that became the slide plane. Meteorological and snow-pit data from a nearby (1 km) site are used with the Crocus model to explain the formation of the faceted crystals as follows. A period of slow surface warming followed by rapid cooling created a large temperature gradient in the layer near the surface of the snow cover which formed a thin layer of faceted crystals near the surface. The large gradient remained as the layer became buried and the faceted crystals survived in the snow cover for 9 days until increasing load from snow accumulation led to failure and the avalanche occurred.

Keywords: **Snow metamorphism, faceted crystals, snow avalanches, Crocus model**

1 Introduction

A snow cover is generally composed of layers of different types of snow. The differences are due to variations in the initial precipitation and variations in the subsequent metamorphism due to meteorological conditions and the surrounding snow layers. Each layer is more or less homogeneous and has its own physical properties. *Weak layers*, which are those of relatively low shear strength, have long been of interest to avalanche researchers since they frequently becoming slide planes.

*jim@orange.lowtem.hokudai.ac.jp

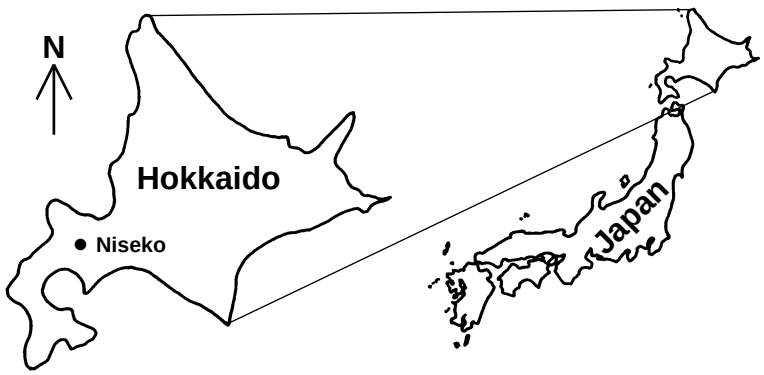

Figure 1: Map showing the location of Niseko in Japan (N 42' 52" E 140' 42")

Weak layers are often comprised of faceted crystals and these can be divided into three types [Birkeland, 1998]: *surface-hoar crystals* that form on the snow surface, *depth-hoar crystals* that form deep in the snow cover often near the ground and *near-surface faceted crystals* that form just under the snow surface. Depth-hoar [Giddings and LaChapelle, 1961, Bradley et al., 1977, Perla, 1978, Marbouty, 1980, Sturm and Benson, 19 Akitaya, 1974] and surface-hoar [Lang et al., 1984, Colbeck, 1988, Hachikubo et al., 1994, Hachikubo and Akitaya, 199 Hachikubo and Akitaya, 1997, Davis et al., 1996] are well known and have received a great deal of study. Near-surface faceted crystals have until recently received much less attention and are often classified as depth-hoar. [Akitaya and Shimizu, 1987] observed quick growth of faceted crystals in the near-surface layer and [Colbeck, 1989] simulated the high growth rate of faceted crystals near the snow surface. [Fukuzawa and Akitaya, 1993] reported near-surface faceted crystals developed largely because of internal warming and melting beneath the snow surface during the day, and radiation cooling at night[1]. This process is called *diurnal recrystallisation* by [Birkeland, 1998] who also describes two other processes leading to the formation of near-surface faceted crystals and defined them as snow crystals formed by near-surface vapor pressure gradients resulting from temperature gradients near the snow surface. Prediction of the formation of near-surface faceted-crystal weak layers using meteorological data is obviously of great practical benefit to avalanche forecasters as well as providing an opportunity for testing theoretical models with physical data.

[Fierz, 1998] compared observations of snow cover temperature and stratigraphy in near-surface layers, in particular the formation of near-surface faceted crystals and their subsequent metamorphosis. He compared the data with two different snow cover models Crocus and DAISY [Bader and Weilenmann, 1992]. This paper compares snow cover data before and immediately after the 28th January 1998 Niseko (Fig. 1) avalanche with the Crocus model for the same period.

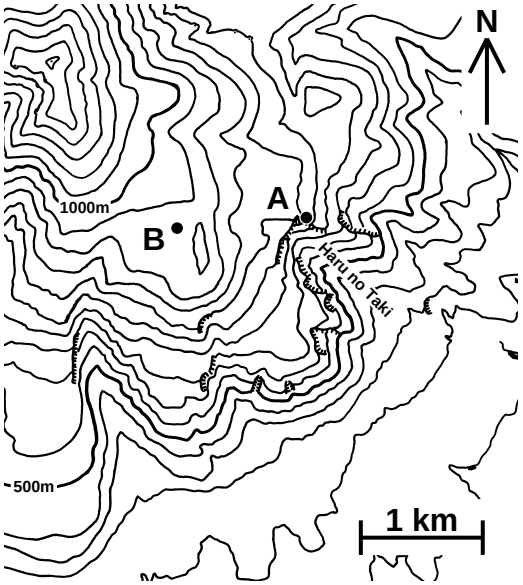

Figure 2: Map showing the location of the observation sites A and B. Contours are every 50 m. The avalanche started near A and ran down the valley Haru no Taki (Spring Waterfall).

2 Observations

2.1 Site and Method

On the morning after the avalanche (29th January) a snow-pit was dug on the fracture line of the avalanche (site A Fig. 2, 820m a.s.l.). The grain shape, grain size, snow density and snow temperature were measured every 0.1 m. The shear strength, using a shear frame, was measured where weak layers were suspected. At a location about 1 km distant (site B Fig. 2, 930m a.s.l.) snow-pit and meteorological measurements were regularly carried out throughout the winter. Air and snow surface temperature, wind speed, solar radiation, snow depth and intensity of snowfall were measured and recorded using a digital data logger every hour. The snowfall counter only measures solid particles and cannot detect liquid precipitation The meteorological instruments are summarized in Table 1.

2.2 Results

The meteorological data (site B) from 17th to 28th are shown in Fig. 3. During the 17th and 18th the air and the snow surface temperature gradually increased to near 0 °C by midnight. A low pressure front then arrived and the air and surface temperatures dropped to around −15 °C in 24 hours. Over the following ten days the temperature remained low between −10 °C and −15 °C. The wind speed was under 7 ms^{-1} for the whole period.

[1] NB this paper refers to near-surface faceted crystals as depth hoar

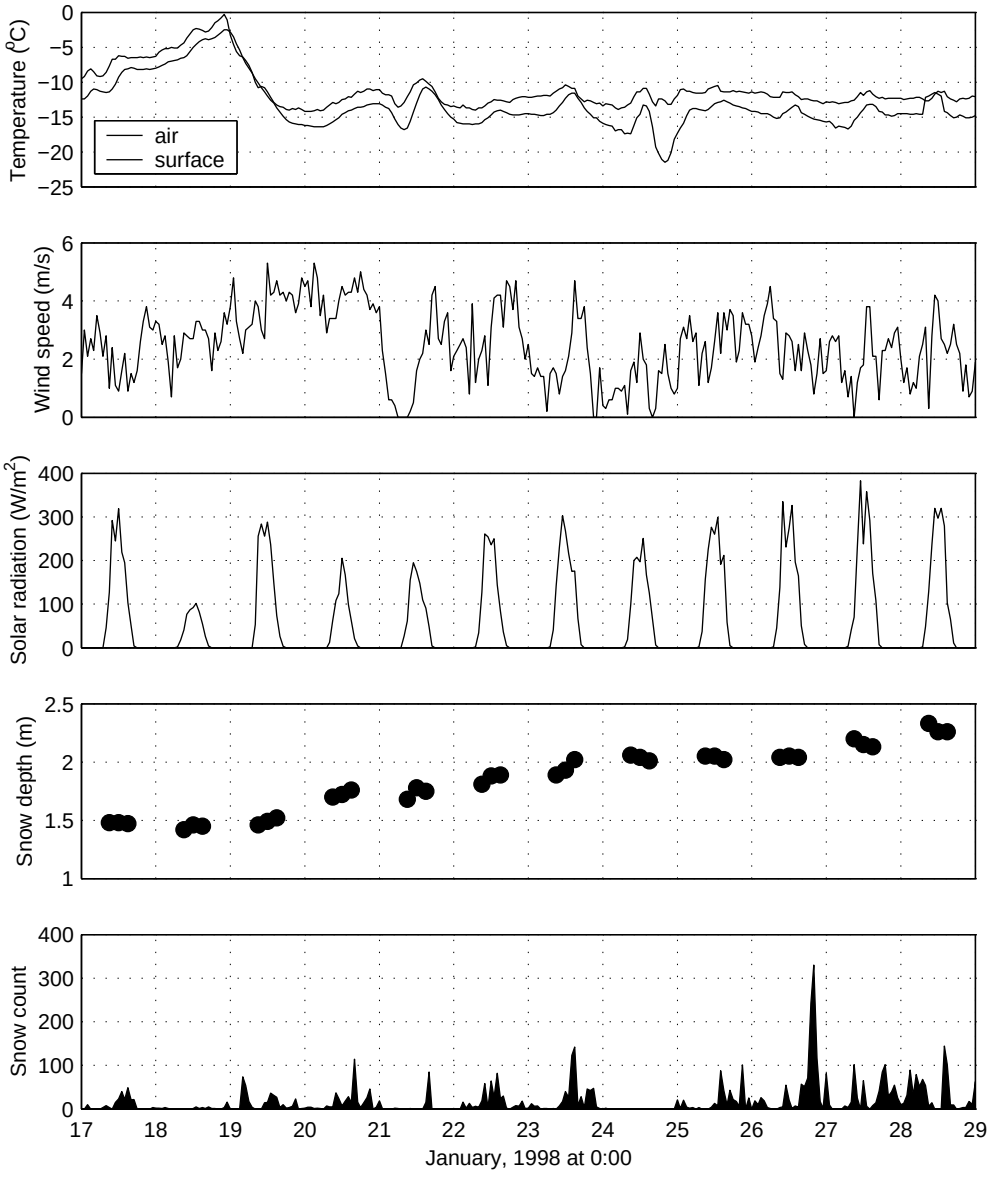

Figure 3: Meteorological data at the site B from 17th to 29th January, 1998.

Measured property	Accuracy	Instrument type	Instrument specification
Air temperature	$\pm 0.1\,^{\circ}\mathrm{C}$	Platinum resistance	VAISALA HMP-35D
Snow surface temperature	$\pm 2\,^{\circ}\mathrm{C}$	Infrared thermometer	HORIBA IT-340W
Humidity	$\pm 3\,\%\mathrm{RH}$	Capacitive sensor	VAISALA HMP-35D
Wind speed	$\pm 0.5\,\mathrm{m/s}$	Windmill anemometer	KDC-S4JR
Shortwave solar radiation	$\pm 5\,\%$	Pyranometer	EKO MS-100
Snow depth	$\pm 0.01\,\mathrm{m}$	Solar cells	KONA KDC-S6
Snow count	not quantified	Infrared reflectance type	SAKATA PC-01

Table 1: Instrumentation

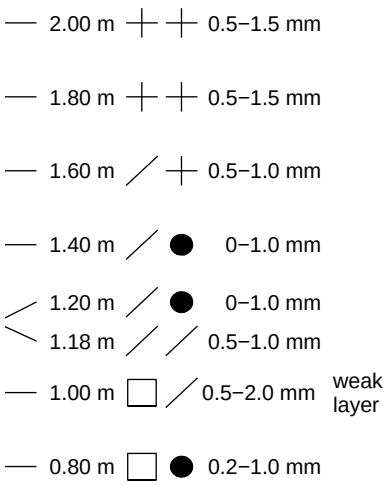

Figure 4: Observed grain profile at site A on 29th January, 12:00, 1998

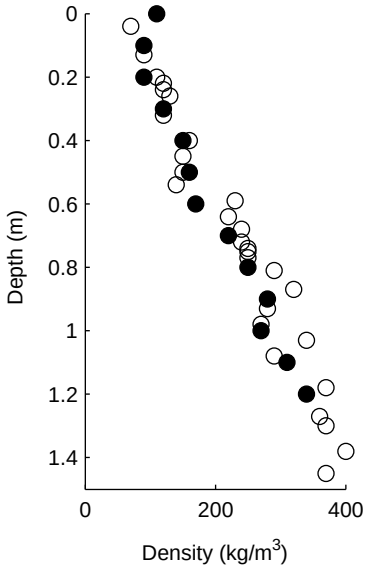

Figure 5: Observed density profile at site A • (29th January) and site B ∘ (27th January).

Snow-pit data from site A are shown in Fig. 4 and Fig. 5. There is a weak layer composed of faceted crystals at a depth of 1m. These crystals were morphologically distinct from depth hoar and surface hoar. The thickness of the weak layer was 10–20 mm, and the grain size was 0.5–2 mm. The shear stress failure (measured using a shear frame) for this weak layer was 3.1 kPa, the slope angle was 34 °C and the weight of snow was 1.45 kPa thus the snow stability index [McClung and Schaerer, 1993] was

$$\frac{3.1\,\mathrm{kPa}}{1.45\,\mathrm{kPa}\,\sin(34^\circ)} = 3.8. \tag{1}$$

This value is not so small, but slab avalanches can start when the stability factor is as high as 4 [Roch, 1966]. The layer may also have stabilised in the twenty-four hours after the avalanche until the observations. The top 0.6 m of the snow cover was approximately homogeneous low density (below $200\,\mathrm{kg\,m^{-3}}$) snow that fell in the two days before the avalanche. This agrees with the meteorological data (Fig. 3) showing that the snow fell under low wind condition. Although there was a relatively weak layer of partly decomposed particles at 0.84 m this layer did not fail. There were no slabs in the snow cover consistent with the low wind speeds.

Snow-pit data from site B are shown for 17th, 22nd and 27th January in Fig. 6. The density profiles and crystal classification at both sites A and B are similar (see Fig. 4 and Fig. 5) confirming that the sites have similar micro-climates. In particular the same faceted crystals weak layer that caused the avalanche was observed at site B on 27th January at a depth of between 0.95 m-1.01 m.

A thin ice layer was observed at site B (Fig. 6) on the 22nd and 27th but not on the 17th. This was probably formed at the warmest time around midnight 19th by surface melting or rime deposition. This does not contradict the meteorological data that shows the surface temperature was never above 0 °C since the sensor error (±2 °C) is large. The snow count sensor cannot distinguish between rime and snow-melt because it only measures solid precipitation. Since the failed weak

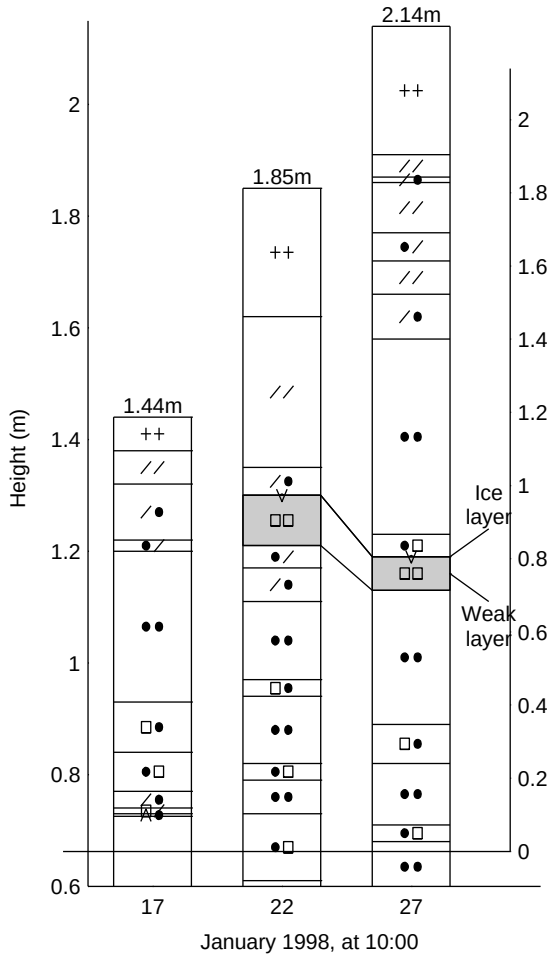

Figure 6: Observed profiles at the site B on 17th, 22nd and 27th January, 1998.

layer was directly below the ice layer it is clear that the weak layer developed from the 0.15 m of snow that fell on the 17th and 18th. However this ice layer did not exist at site A indicating that the sites are not identical. This is possibly because of the different aspect and inclination leading to differences in the surface temperature, or more likely because the different topographies lead to a longer exposure to rime producing fog at site B.

3 Numerical Simulation

3.1 Description of the simulation

Crocus [Brun et al., 1989, Brun et al., 1992] is a numerical model of snow cover developed for avalanche forecasting by Meteo-France. Given initial conditions (the snow cover) and boundary conditions (meteorological data at the surface) it can simulate the subsequent time-evolution of the snow cover. Crocus requires the specification of nine meteorological conditions; air temperature, relative humidity, wind speed, precipitation (rate and phase), incoming long-wave radiation, direct and diffuse short-wave radiation and cloudiness.

Crocus was used to simulate the evolution of the snow cover between the 17th and the 29th — the period from just before the snow in the weak layer fell to just after the avalanche occurred. The snow pit data from the 17th (site B) was used for the initial conditions (see Table 3). No data was available for the bottom 0.74 m and this was assumed to be rounded grains with mean temperature averaged from the measured temperature at 0.74 m and the assumed temperature of 0 °C on the ground. Air temperature, relative humidity, wind speed precipitation and diffuse short-wave radiation were taken directly from the meteorological instruments. The instruments did not measure direct short-wave radiation or incoming long-wave radiation, but since a local meteorological observatory (Kutchan 10 km northeast from site A) showed that it was cloudy for this time direct short-wave radiation was assumed to be zero. Incoming long-wave radiation was calculated from a heat balance using the measured snow surface temperature.

3.2 Modifications to Crocus

Crocus release 2.2.1 (26th Feb 1997) was used for the simulation with some small modifications described in this section. The snow profile was output every hour instead of every day and the profile data was processed using 5 decimal places. Modification were made to `agreg.f`, `modprof.f` and `neige.f` so that the creation of new layers, the aggregation of layers and the splitting of existing layers could be tracked. The maximum number of layers was increased from 50 to 200 so that aggregation of layers only occurred when they had similar physical properties.

One modification was also made that effects the physics of Crocus. When a layer is split in to two the properties for the new layers are calculated from the old layer assuming it to be homogeneous. This is a good approximation for density, crystal type, et cetera as the defining property of a snow layer is that it is roughly homogeneous. However, in general the temperature varies linearly across a layer and assigning the same temperature to the two new layers is inaccurate and results in very large spikes in the temperature gradient. A simple modification to overcome this problem is as follows.

Let the thickness of the layer be $4\delta x$ centred at x and its mean temperature be t. Crocus splits new layers into two equal halves so that the new layers have thickness $2\delta x$ and are centred at $x \pm \delta x$ with temperature $t_\pm$. Conservation of heat energy implies that $4\delta x t = 2\delta x t_+ + 2\delta x t_-$. Write the

new temperatures as $t_\pm = t \pm \delta x\, \delta t$ then δt is the temperature gradient at x. Crocus chooses $\delta t = 0$, but a more physical choice is to choose d^2t/dx^2 continuous. If the centres of the layers above and below relative to x are x_u and $-x_l$, and the mean temperatures are t_u and t_l respectively then

$$\left(\delta t - \frac{t - t_l - x\delta t}{x_l - x}\right)(x + x_l)^{-1} = \left(\frac{t_u - t - x\delta t}{x_u - x} - \delta t\right)(x_u + x)^{-1} \tag{2}$$

$$\delta t = \frac{(x_u^2 - x^2)(t - t_l) + (x_l^2 - x^2)(t_u - t)}{(x_l + x_u)(x_l x_u - x^2)}. \tag{3}$$

Thus this is equivalent to choosing the temperature gradient at x to be a linear interpolation of the temperature gradients above and below the new layers. This modification was made to the file `modpro.f`.

The modified version of Crocus make it easy to track the evolution of layers though the snow cover and to study their properties. In particular the temperature gradients experienced by a layer can be studied. This is useful because even if the metamorphism modeled by Crocus is inaccurate the temperature profile is based on the well understood physics of heat conduction. Classification of Crocus crystal types is performed according to Table 2. Only crystals with size less than 0.5 mm are included since only these occurred in this simulation.

3.3 Crocus model results

dendricity	sphericity	history	crystal type	
(0.85,1)	(0,1)	0	++	fresh snow
(0.65,0.85)	(0,1)	0	+/	
(0.35,0.65)	(0,1)	0	//	decomposed and fragmented
(0.15,0.35)	(0,0.5)	0	/□	
(0.15,0.35)	(0.5,1)	0	/•	
(0,0.15)	(0,0.2)	0,1	□□	faceted crystals
(0,0.15)	(0.2,0.5)	0,1	□•	
(0,0.15)	(0.5,0.8)	0,1	•□	
(0,0.15)	(0.8,1)	0,1	••	rounded grains
0	(0.0,0.5)	2,3,4,5	∘□	
0	(0.5,1.0)	2,3,4,4	∘∘	wet grains

Table 2: Crocus model crystal classification adapted from users manual version 2.2 [Brun et al., 1992]) for dendritic and non-dendritic types for sizes less than 0.5 mm. Types from [Colbeck et al., 1990] are as follows: + = 1, / = 2, •=3, □ = 4 and ∘ = 6

The simulated snow cover from the 17th to the 29th is shown in Figs.7 and 8. The model agrees well with the actual snow pack on the 22nd and 27th (Fig. 6). However, the snow depth is overestimated by about 0.3 m and the thin ice layer was not reproduced by Crocus. This suggests that the ice layer was a rime deposit since the model does not include rime deposition, but does include surface melting. [Fierz, 1998] found similar problems with Crocus. In his measurements there was also a thin crust above the faceted crystals that Crocus failed to produce and he also found problems with the snow depth prediction as did [Brun et al., 1992].

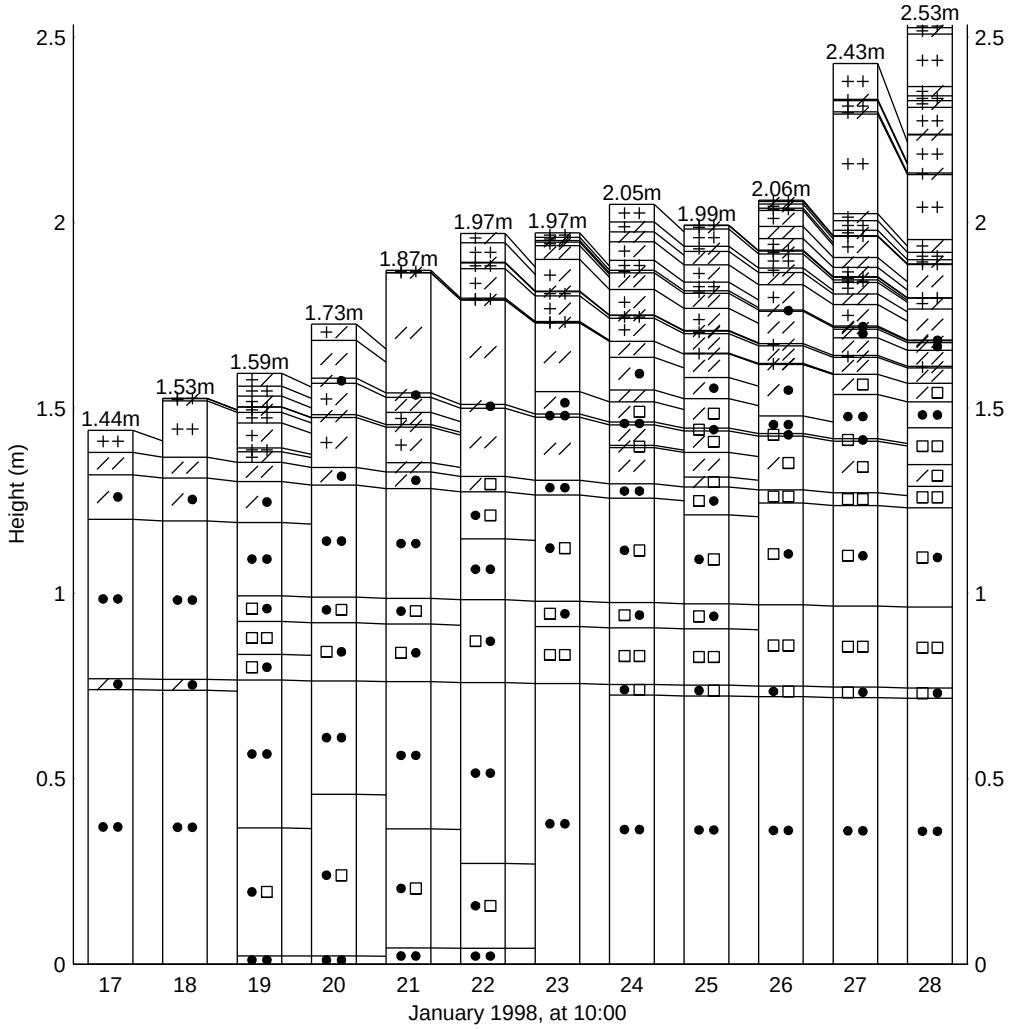

Figure 7: Simulated profile of snow crystal type from 17th to 29th.

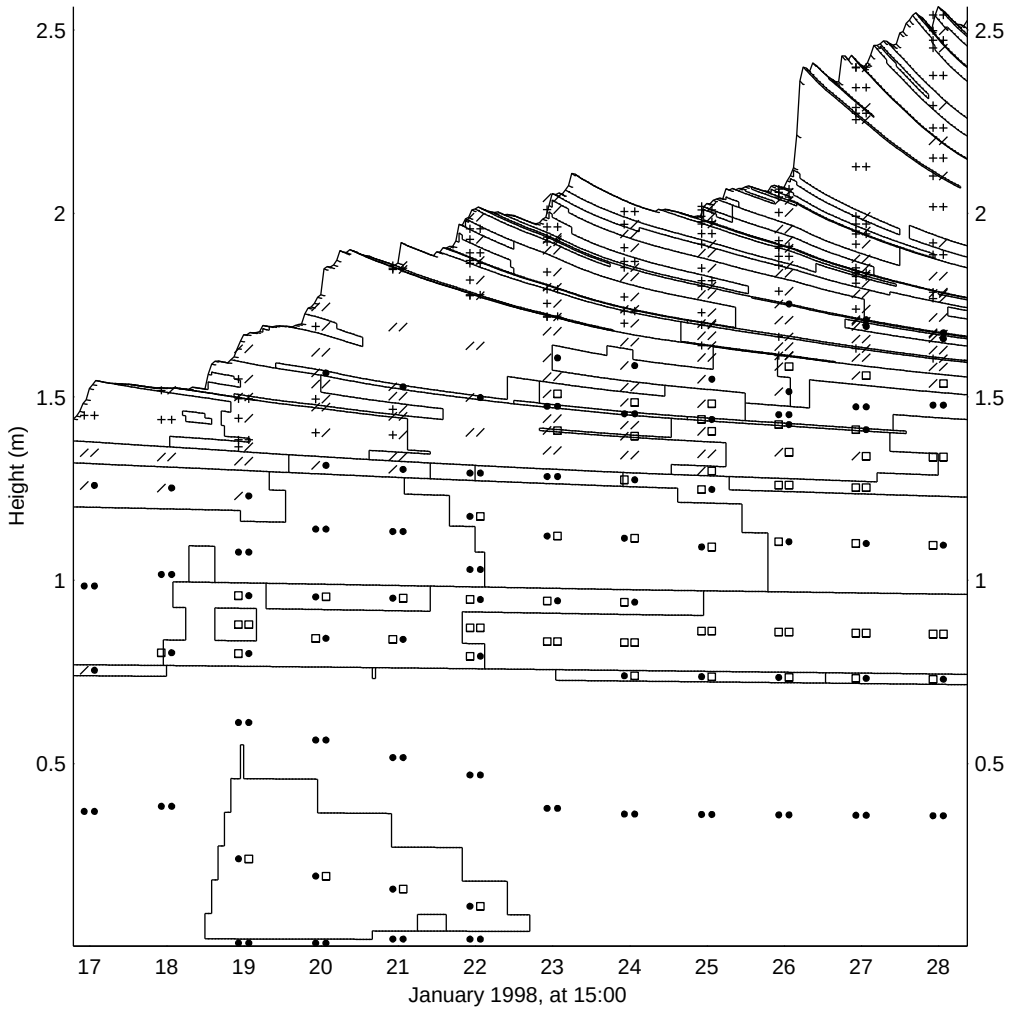

Figure 8: Simulated profile of snow crystal type from 17th to 29th.

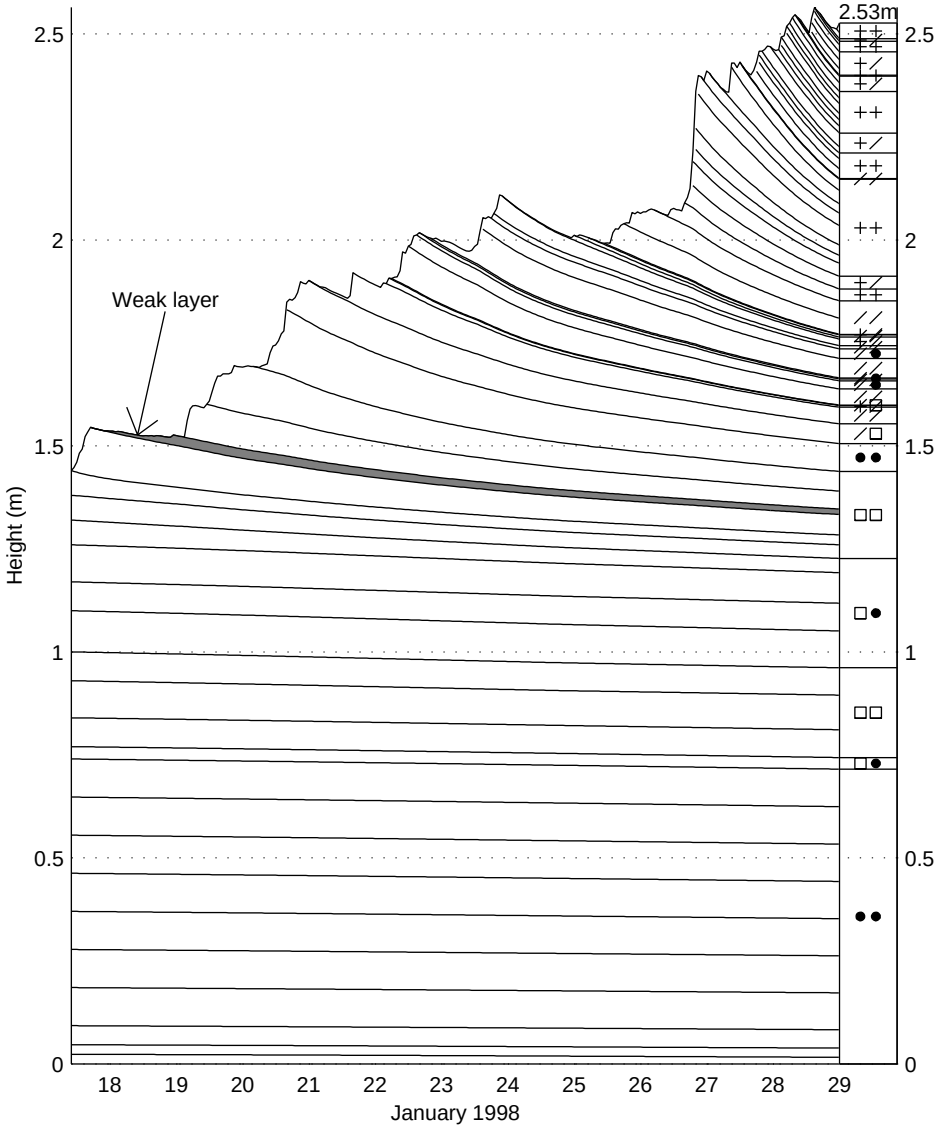

Figure 9: Simulated on January 19th and where the layers came from

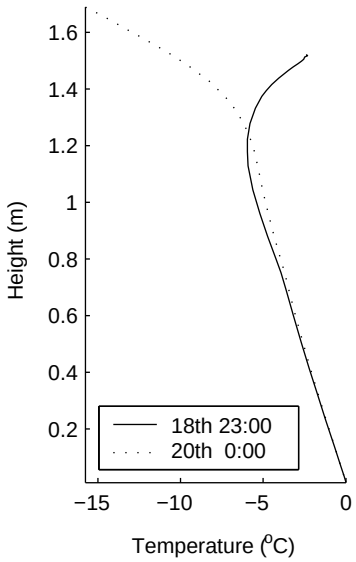

Figure 10: Simulated temperature profile.

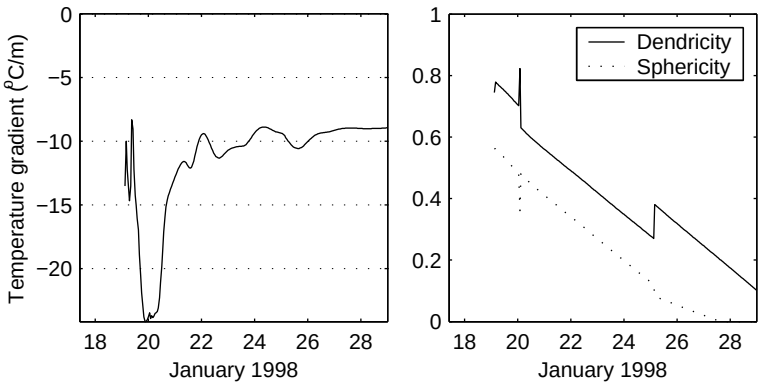

Figure 11: Left: Temperature gradient across the weak layer. Right: Dendricity and Sphericity of the weak layer.

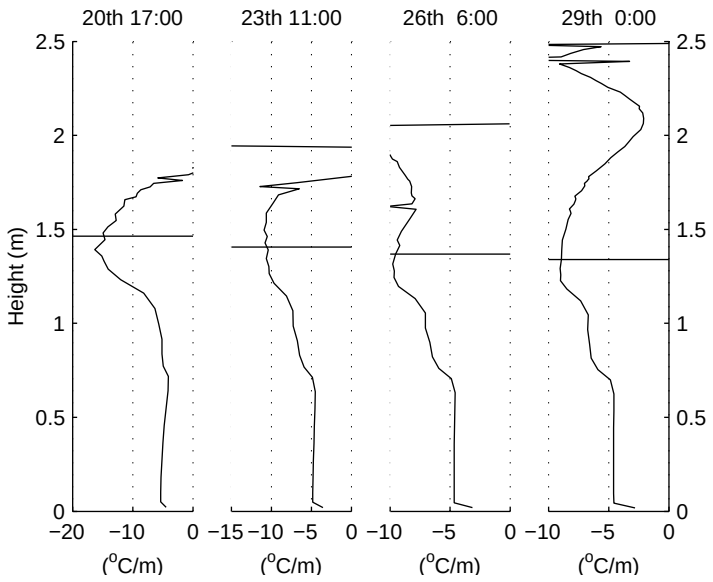

Figure 12: Simulated temperature gradient profile at four times. Solid horizontal line indicates the position of the weak layer.

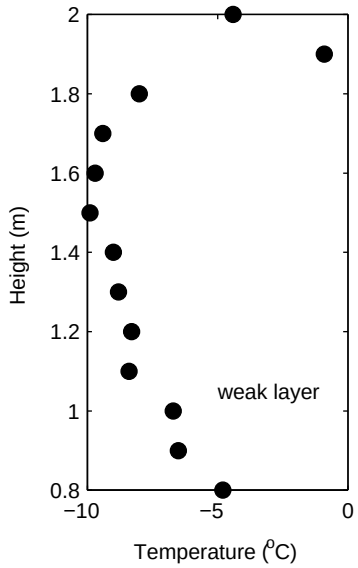

Figure 13: Observed temperature profile at site A on 29th January, 12:00

Figure 9 shows the final snow cover and the settling of the simulated layer boundaries. The weak layer is also marked and the temperature gradient and crystal properties of this layer are shown in Fig. 11. This layer corresponds to the snow on the surface between 17:00 on the 17th and 3:00 on the 19th. The high temperature gradient caused by the falling surface temperature on the 19th can be clearly seen. The temperature gradient increased in magnitude to $-24\,^{\circ}\mathrm{C/m}$ and remained larger than $-9\,^{\circ}\mathrm{C/m}$ up until the avalanche on the 28th. In the Crocus model kinetic growth occurs when the temperature gradient is larger than $5\,^{\circ}\mathrm{C/m}$. Thus this layer of snow was slowly changing to faceted crystals for the entire period, but the gradient was only briefly large enough for faceted crystal large than 0.5 mm to form (this only occurs when the gradient is larger than $-15\,^{\circ}\mathrm{C/m}$.) This is shown in the lower figure. The discontinuity of the dendricity and the sphericity is a simulation artifact caused by Crocus merging layers with similar properties. The final state reached by this layer corresponds to almost perfectly faceted crystal less than 0.5 mm in size.

The existence of the temperature gradient can be explained as followed. Figure 10 show the simulated temperature profile at 23:00 on the 18th and midnight on the 20th — the times of maximum difference. As the surface temperature fell and new snow cold snow was deposited a large kink in the temperature profile was generated at around 0.4 m depth. Fresh snow continued falling insulating the warmer snow deeper in the snow cover. Figure 12 shows the evolution of the temperature kink and the location of the weak layer. The kink gradually spreads out and reduces but is still clearly visible after ten days. It persists for so long because The initial warm period was long enough for the top 0.4 m of the snow pack to warm up (Fig. 10) and then be buried by more than 1 m of cold snow. Figure 13 shows the measured temperature profile at A. There is only rough agreement with the simulated snow cover, but the data does show a large temperature gradient ($17\,^{\circ}\mathrm{C/m}$) at the weak layer — the temperature changes $-8.4\,^{\circ}\mathrm{C}$ to $-6.7\,^{\circ}\mathrm{C}$ in 0.1 m.

4 Discussion

For dry snow with dendricity > 0 and temperature gradient $|\Delta T| > 5\,^{\circ}\mathrm{C/m}$ Crocus predicts that the crystals become faceted according to the rate law

$$\frac{d\text{dendricity}}{dt} = \frac{d\text{sphericity}}{dt} = -2 \times 10^8 |\Delta T|^{0.4} \exp -\frac{6 \times 10^3}{T}, \tag{4}$$

where time is measured in days. The end state with dendricity and sphericity both zero corresponds to faceted crystals of size 0.4 mm. If the gradient is above $15\,^{\circ}\mathrm{C/m}$ the grains increase in size and evolve towards depth hoar. If the gradient falls below $5\,^{\circ}\mathrm{C/m}$ The grains increase in sphericity and evolve towards rounded crystals. If Eq. 4 if integrated for the weak layer (Fig. 11) it shows that dendricity and sphericity should decrease by about 0.7 and this of course agrees with the simulation.

Though the Crocus simulation shows qualitative agreement with the measurements and correctly predicts the formation of a weak layer in the correct place (adjusting for the depth miscalculation). The characteristics are somewhat different. Crocus predicted smaller grains (< 0.5 mm) in a thick weak layer (0.1 m) in contrast to the observed large grains (0.5–2 mm) in a thin (0.01 m) layer. Since Crocus predicted the snow cover was about 25% deeper (2.5 m instead of $2m$ at site A) the temperature gradient in the weak layer should be about 25% larger. Since the rate dependence on temperature gradient is fairly weak however this increases the rate by only around 9%. This is enough to make the final crystals fully faceted (dendricity and sphericity zero) but they will not evolve towards large faceted crystals since the gradient is less than $15\,^{\circ}\mathrm{C/m}$ except from the 19th to the 21st. For the crystals to have become fully faceted in this time temperature gradients of around

300 °C/m would have been necessary. There are three possible explanations. The simplest is that the crystal growth laws in Crocus are wrong and large faceted crystals can develop even in temperature gradients of 9 °C/m. This seems unlikely as the Crocus model is based on detailed experiments of crystal metamorphism. Another possibility is that Crocus describes the metamorphism of the weak layer correctly and the discrepancy is natural variation. This also seems unlikely as the weak layer in the snow cover was thin and distinct from surrounding layers in contrast to the simulation. The most likely reason however is that the weak layer is the result of near-surface faceted crystals formed on the 19th as the temperature rapidly plunged. This explanation also agrees better with the snow-pit data showing a weak layer of faceted crystals existing by the 22nd (Fig. 6). Crocus cannot resolve large near-surface temperature gradients since it lacks the spatial resolution and a micro-climate model. Thus it cannot account for this possibility. The thinness of the layer also fits this hypothesis, and if such a layer had formed the temperature gradients higher than 5 °C/m predicted by Crocus ensure that it would have survived. The weak layer then remained in the snow pack until the increasing weight of the snow cover caused failure.

Birkeland (1998) classified processes associated with the formation of weak layers of faceted crystals near the snow surface into the following three types: *radiation recrystallisation*, *melt-layer recrystallisation* and *diurnal recrystallisation*. Radiation recrystallisation is ruled out because the sky was overcast. Melt-layer recrystallisation can not have been the cause since there was no melt layer in the snow cover at the site of the avalanche, though it may have had an effect at site B. Diurnal recrystallisation refers to gradients induced by temperatures differences between day and night. Since the warmest temperatures were at midnight and the temperatures dropped during the day neither is this the explanation. Instead a fourth case is necessary, covering the case when synoptic weather conditions cause large temperature variation. Under the right conditions low-density surface snow can change to near-surface faceted crystal in only one night[Birkeland, 1998] and these crystals were then preserved in the snow cover until the avalanche.

5 Conclusions

Despite its limitations Crocus is a valuable tool for studying the evolution of snow covers. Though it did not predict exactly the weak layer that caused this avalanche it did predict a weak layer at the correct depth and its results confirm that large faceted crystals in the layer would have been preserved. Thus if expert knowledge of near-surface faceted crystal formation is used in conjunction with Crocus avalanches such as this can be predicted.

A Acknowledgments

We would like to thank Niseko Higashiyama Ski Area and Niseko Hirafu Ski Area for their cooperation. We are also grateful to A. Shinya for providing logistic support. Crocus was used under license from Meteo-France. This research was supported by the Fund for Avalanche Research of the Ministry of Education, Science, Sports and Culture, Japan. One of the authors (JM) was supported by Fellowships from the Japanese Society for the Promotion Science and The European Union.

Depth (m)	Temperature (°C)	Density (kg/m^3)	g1	g2
1.44	-5.93	0.04	-99	50
1.41	-6.61	0.16	-90	45
1.38	-7.96	0.14	-50	50
1.32	-8.48	0.15	-25	60
1.26	-8.02	0.23	-25	60
1.22	-7.76	0.23	-25	75
1.20	-7.55	0.24	-12	80
1.17	-7.10	0.32	-10	82
1.10	-6.35	0.28	-10	80
1.00	-5.60	0.32	-10	50
0.93	-5.07	0.30	-12	35
0.84	-4.50	0.34	-10	50
0.77	-4.08	0.33	-25	60
0.74	-2.03	0.40	-1	99

Table 3: Initial conditions for Crocus simulation. The history variable and liquid water content were zero for all layers.

Postscript

The software used for producing the figures in this paper and for analysing the Crocus simulations as well as a detailed list of the modifications is available from one of the authors web site: http://duvel.lowtem.hokudai.ac.jp/~jim/crocus.

References

[Akitaya, 1974] Akitaya, E. (1974). Studies on depth hoar. *Low Temp. Sci. Ser. A*, 26:67.

[Akitaya and Shimizu, 1987] Akitaya, E. and Shimizu, H. (1987). Observations of weak layers in a snow cover. *Low Temp. Sci. Ser. A*, 46:67–75. in Japanese with English summary.

[Bader and Weilenmann, 1992] Bader, H.-P. and Weilenmann, P. (1992). Modeling temperature distribution energy and mass flow in a (phase-chnaging) snowpack. i. model and case studies. *Cold Reg. Sci. Tech.*, 20(2):157–181.

[Birkeland, 1998] Birkeland, K. W. (1998). Terminology and predominant processes associated with the formation of weak layers of near-surface faceted crystals in the mountain snowpack. *Arct. Alp. Res.*, 30:193–199.

[Bradley et al., 1977] Bradley, C. C., Brown, R. L., and Williams, T. (1977). On depth hoar and the strength of snow. *J. Glaciol.*, 18(78):145–147.

[Brun et al., 1992] Brun, E., David, P., Sudul, M., and Brugnot, G. (1992). A numerical model to simulate snow-cover stratigraphy for operational avalanche forcasting. *J. Glaciol.*, 38(128):13–22.

[Brun et al., 1989] Brun, E., Martin, E., Simon, V., Gendre, C., and Coleou, C. (1989). An energy and mass model of snow cover suitable for operational avalanche forecasting. *J. Glaciol.*, 35(121):333–342.

[Colbeck et al., 1990] Colbeck, S., Akitaya, E., Armstrong, R., Gubler, H., Lafeuille, J., Lied, K., McClung, D., and Morris, E. (1990). *The international classification for seasonal snow on the ground.* International Association of Scientific Hydrology, Wallingford, Oxfordshire. International Commission on Snow and Ice.

[Colbeck, 1988] Colbeck, S. C. (1988). On the micrometeorology of surface hoar growth on snow in mountanous areas. *Bound.-Lay. Meteorol.*, 44:1–12.

[Colbeck, 1989] Colbeck, S. C. (1989). Snow-crystal growth with varying surface temperatures and radiation penetration. *J. Glaciol.*, 35(119):23–29.

[Davis et al., 1996] Davis, R. E., Jamieson, B., Hughes, J., and Johnston, C. (1996). Observations on buries surface hoar — persistent failure planes for slab avalanches in bc. In [Jamieson, 1996], pages 81–85.

[Fierz, 1998] Fierz, C. (1998). Field observation and modelling of weak-layer evolution. *Ann. Glaciol.*, 26:7–13.

[Fukuzawa and Akitaya, 1993] Fukuzawa, T. and Akitaya, E. (1993). Depth-hoar crystal growth in the surface layer under high temperature gradient. *Ann. Glaciol.*, 18:39–45.

[Giddings and LaChapelle, 1961] Giddings, J. C. and LaChapelle, E. R. (1961). The formation rate of depth hoar. *Alta Avalanche Study Centre Project C*, Progress Report No. 2.

[Hachikubo and Akitaya, 1997] Hachikubo, A. and Akitaya, E. (1997). Effect of wind on surface hoar growth on snow. *J. Geophys. Res.*, 102(D4):4367–4373.

[Hachikubo and Akitaya, 1998] Hachikubo, A. and Akitaya, E. (1998). Daytime preservation of surface hoar crystals. *Ann. Glaciol.*, 26:22–26.

[Hachikubo et al., 1994] Hachikubo, A., Fukuzawa, T., and Akitaya, E. (1994). Formation rate of surface hoar crystals under various wind velocities. In *International Snow Science Workshop, 30 October – 3 November 1994, Snowbird, Utah*, pages 132–137, Snowbird, UT, P.O. Box 49. American Association of Avalanche Professionals.

[Jamieson, 1996] Jamieson, J. B., editor (1996). *International Snow Science Workshop, 6–10 October 1996, Banff, Canada*, P.O. Box 2759, Revelstoke, B.C. Canadian Avalanche Association.

[Lang et al., 1984] Lang, R. M., Leo, B. R., and Brown, R. L. (1984). Observations on the growth processes and strength characteristics of surface hoar. In *Snow Science Workshop, Aspen, Colorado*, pages 188–195. American Association of Avalanche Professionals.

[Marbouty, 1980] Marbouty, D. (1980). An experimental study of temperature-gradient metamorphism. *J. Glaciol.*, 26(94):303–312.

[McClung and Schaerer, 1993] McClung, D. and Schaerer, P. (1993). *The Avalanche Handbook.* The Mountaineers, Seattle, Washington.

[Perla, 1978] Perla, R. (1978). Temperature-gradient and equi-temperature metamorphism of dry snow. In *Deuxième Recontre Internationale sur la Neige et les Avalanches*, Grenoble, France 12–14 April, 1978. Association Nationale pour l'Étude de la Neige et des Avalanche.

[Roch, 1966] Roch, A. (1966). Les d'clenchements d'avalanches. *Int. Ass. Sci. Hydrol. Publ.*, 69:182–195.

[Sturm and Benson, 1997] Sturm, M. and Benson, C. S. (1997). Vapour transport, grain growth and depth-hoar development in the subarctic snow. *J. Glaciol.*, 43(143):42–59.